Horizontal flows in the atmospheres of chemically peculiar stars

A. ud-Doula^{1,*}, J. Krtička², and B. Kubátová³

- Penn State Scranton, 120 Ridge View Drive, Dunmore, PA 18512, USA e-mail: asif@psu.edu
- Department of Theoretical Physics and Astrophysics, Masaryk University, Kotlářská 2, CZ-611 37 Brno, Czech Republic
- Astronomical Institute of the Czech Academy of Sciences, Fričova 298, 251 65 Ondřejov, Czech Republic

ABSTRACT

Context. Classical chemically peculiar stars exhibit atmospheres that are often structured by the effects of atomic diffusion. As a result of these elemental diffusion and horizontal abundance variations, photospheric temperature varies at a given height in the atmosphere. This may lead to horizontal flows in the photosphere. In addition, the suppression of such flows by magnetic field can alter the

Aims. Using a simplified model of such a structured atmosphere and 2D MHD simulations of a typical He-rich star, we examine atmospheric flows in these chemically peculiar stars which often are strongly magnetic.

Methods. We use Zeus-MP which is a Fortran 90 based publicly available parallel finite element modular code.

Results. We find that for non-magnetic stars of spectral type BA, atmospheric flow related to horizontal temperature gradient can reach 1.0 km s⁻¹ yielding mixing timescale of order of tens of days. For the magnetic counterparts, the flow speeds are an order of

Conclusions. Magnetic field can influence the dynamics in atmospheres significantly. Strong horizontal magnetic field inhibits flow in the vertical direction, while strong vertical magnetic field can suppress horizontal atmospheric flow preventing elemental mixing.

Key words. stars: magnetic field – stars: chemically peculiar – stars: early-type – circumstellar matter – stars: variables: general

Context. Classical chemically peculiar stars exhibit atmospheres the of these elemental diffusion and horizontal abundance variations, possible the processes.

Aims. Using a simplified model of such a structured atmosphere atmosphere flows in these chemically peculiar stars which often a Methods. We use Zeus-MP which is a Fortran 90 based publicly a Results. We find that for non-magnetic stars of spectral type BA reach 1.0 km s⁻¹ yielding mixing timescale of order of tens of day magnitude lower allowing for stratification of chemical elements. Conclusions. Magnetic field can influence the dynamics in atmosphere in the vertical direction, while strong vertical magnetic field can see Key words. stars: magnetic field – stars: chemically peculiar – stational force (Michaud et al. 2011, 2015; Alecian & Stift 2017). In absence of strong mixing, this leads to horizontal and vertical abundance stratification in the outer layers of these stars (Kochukhov & Wade 2010; Kochukhov et al. 2011; Ryabchikova et al. 2016; Grunhut et al. 2017). The rotation of stellar surface strewn with in-homogeneously distributed elements together with frozen-in magnetic field manifests itself in plethora of remarkable phenomena. This includes regular light variability (Faltová et al. 2021; Labadie-Bartz et al. 2023), which stems from the flux frequency redistribution induced by horizontal chemical inhomogeneity (Krtička et al. 2015; Prvák et al. 2015), or radio activity originating from the interaction of a weak stellar wind with strong magnetic field (Leto et al. 2021; Das et al. 2022; Owocki et al. 2022). lar wind with strong magnetic field (Leto et al. 2021; Das et al. 2022; Owocki et al. 2022).

Although many detailed characteristics of chemically peculiar stars can be understood from theoretical models, the processes shaping their surface elemental distribution are not fully understood. The diffusion models predict a tight correlation between surface elemental distribution and magnetic field (Alecian & Stift 2017), what is perhaps the case only for some elements (Kochukhov & Ryabchikova 2018). Neither the observed

characteristics of light variations of magnetic chemically peculiar stars do not seem to support a strong correlation between magnetic field and surface abundance distribution (Jagelka et al. 2019). In particular, simulations of light curves based on abundance spots associated with magnetic fields predict a much higher prevalence of double-wave light curves per rotation period than is observed.

Although the theoretical diffusion models and abundance distributions inferred from observations seem to contradict, any additional process that modifies the surface abundance distribution is likely to be rather weak. This is indicated by stability of the observational characteristics of magnetic chemically peculiar stars. Neither the observed light curves (Hümmerich et al. 2018) nor the underlying surface abundance distribution (Potravnov et al. 2024) seem to show any secular changes. This implies that either the abundance stratification has reached an equilibrium state or that the forming processes operate on a longer timescale (e.g., Alecian et al. 2011).

A better understanding of the diffusion processes can be perhaps gleaned from the analysis of chemically peculiar stars of Am and HgMn type. These stars do not show strong magnetic fields (Makaganiuk et al. 2012; Kochukhov et al. 2013; Catanzaro et al. 2016; Blazère et al. 2020) that would impede the interaction of mixing processes and elemental diffusion unlike in the magnetic chemically peculiar stars. This is likely the reason why the rotational light variability in HgMn stars is much weaker than in magnetic chemically peculiar stars. As a result, the light variability of a fraction of HgMn stars remained undetected until the age of precise space borne instruments (Kochukhov et al. 2021). Moreover, the connection between the light variability and surface abundance inhomogeneities is not well established.

^{*} corresponding author

Despite this, in some of these stars it was possible to detect secular changes of surface elemental distribution of yet unknown origin (Briquet et al. 2010; Korhonen et al. 2013; Prvák et al. 2020).

While the deviations from the axial symmetry of the stellar surface either due to the magnetic fields (Fuller & Mathis 2023) or due to hydrostatic scale-height variations caused by horizontal abundance variations (Krtička et al. 2020) are rather small, other dynamical processes were invoked to provide additional mixing of atmospheres of chemically peculiar stars. Such processes may include turbulence and mass loss (Michaud et al. 2011; Alecian & Stift 2019) or meridional circulation (Michaud et al. 1983).

In addition to these processes, there is a possible mixing process directly linked to peculiarity, which was not studied in detail up to now. As a result of elemental diffusion and induced horizontal abundance variations, the photospheric temperature varies at a given height in the atmosphere. Such horizontal temperature variations exist regardless of the overall constancy of the effective temperature (Molnar 1973) and appear as a result of influence of heavy element abundance on opacity. These temperature variations occurring in the optically thin photospheric layers are rather weak (on the order of 10 - 100 K), and are connected with surface brightness variations and light variability (Khan & Shulyak 2007; Krtička et al. 2007, 2012).

The variation in temperature at a given height within the atmospheres of chemically peculiar stars implies that pressure is likewise non-uniform at the same altitude (e.g. Peterson 1970). In such cases, horizontal pressure differences generate weak lateral flows analogous to atmospheric winds on Earth. Given the complex surface abundance patterns in chemically peculiar stars, the resulting flow induced by these pressure gradients represents a complex three-dimensional problem. Numerical modeling of this phenomenon is challenging due to the substantial difference in the horizontal and vertical extents of the flow, with significant disparities in scale making such simulations computationally intensive. Furthermore, the structure of the flow varies from star to star due to unique abundance stratifications across each stellar surface.

To develop a clearer physical understanding of this phenomenon, we address a simplified model assuming an initial linear temperature gradient in two dimensions directly over the region of chemical peculiarity. This approach enables us to estimate the intensity of the pressure gradient-driven flow while capturing essential dynamics. Additionally, we introduce uniform magnetic fields of different orientations and strengths into our simulations to explore the potential damping effects on these flows, which is particularly relevant in the atmospheres of the chemically peculiar magnetic stars, where magnetic suppression of flow could alter the transport processes.

In section 2 we discuss the specifics of our numerical methods. We then present our results in section 3. We follow this by a brief discussion in section 4 before a short summary and future work in section 5.

2. Numerical Methods

To model flows stemming from the horizontal temperature gradients, we set up a 'box-in-a-star' simulation of the hydrostatic stellar atmosphere wherein a chemical spot with varying temperature is mimicked by a region with temperature ΔT higher than the effective temperature $T_{\rm eff}$ of the star.

We use the publicly available hydrodynamic code Zeus-MP (Hayes et al. 2006) to model the atmospheric structure of a chemically peculiar star under a planar approximation. The

stellar parameters used in the simulations here are chosen to approximate a typical magnetic helium-strong star HD 37776 (Mikulášek et al. 2008) and are as follows: mass $M=8~M_{\odot}$, radius $R=4~R_{\odot}$, and effective temperature $T_{\rm eff}=22,000~{\rm K}$. Although we use full energy equation for the gas, we assume adiabatic index $\gamma=1.01$, reflecting nearly isothermal atmospheric conditions.

Table 1. Summary of models with varying magnetic field strengths and orientations.

Model	Magnetic Field (G)	Field Orientation
Non-magnetic	0	-
Weak Field	1	Horizontal, Vertical
Moderate Field	10	Horizontal, Vertical
Strong Field	100	Horizontal, Vertical
Very Strong Field	1000	Horizontal, Vertical

2.1. Initial and boundary conditions

We initialize all our simulations with hydrostatic planar atmosphere with fixed gravitational acceleration $g \equiv G M_*/R_*^2$ and base density $\rho_* = 10^{-8} \text{ g cm}^{-3}$. At time t = 0 s we introduce uniform magnetic field with different strengths and orientations as noted in Table 1.

We include a temperature variation in the form of a chemical spot, specified as a linear temperature increase of $\Delta T = 100 \text{ K}$ at X = 0, symmetric about X = 0 and spanning 5 H_{scale} on both sides, where $H_{\text{scale}} = k_B T/(\mu m_H g) = a^2/g$ is the pressure scale height with isothermal sound speed $a = \sqrt{k_B T/(\mu m_H)} \sim 17 \text{ km s}^{-1}$ where μ is the mean molecular weight and m_H is the hydrogen mass. For the parameters assumed in this work, it amounts to $H_{\text{scale}} \sim 2.1 \times 10^8 \text{ cm}$.

For the horizontal (X) direction, we fix density and pressure to the value appropriate for a hydrostatic atmosphere. We also keep magnetic field components constant. While horizontal component of the velocity is kept at zero value in the interest of numerical stability, the vertical component is allowed to float through linear extrapolation from the two closest zones inside the computational domain.

At the outer boundary, which represents the upper atmosphere, outflow boundary conditions are implemented, allowing all magnetohydrodynamic quantities to vary freely. This boundary is located at approximately $X=10\ H_{\rm scale}$ or about 21,000 km above the stellar surface.

Reflective boundary conditions are imposed along the vertical (z) direction, corresponding to the left and right sides in all subsequent figures. Under these conditions, the parallel components of velocity and magnetic field remain unchanged, while the perpendicular components reverse their direction.

The computational domain spans a total horizontal extent of $20~H_{\rm scale}$, while the vertical extent is half as large, measuring $10~H_{\rm scale}$.

The computational domain is discretized into 128×64 grid zones along the x- and z-directions, yielding approximately 6–7 grid points per scale height ($H_{\rm scale}$). A total of nine models are explored: one non-magnetic reference case and eight magnetic configurations with field strengths of 1, 10, 100, and 1000 G in both horizontal and vertical orientations. Each simulation spans a physical time of 100 ks, corresponding to over 50 sound crossing times, ensuring adequate time for the system to reach equilibrium.

3. Simulation results

3.1. Non-magnetic Model

To establish a basis for comparison across all magnetic models, we first examine the non-magnetic case (0 G). Fig. 1 illustrates the temporal evolution of the non-magnetic model, with panels showing temperature T (left column), horizontal velocity v_x (middle column), and vertical or radial velocity v_z (right column), all in cgs units. Initially, the model is assumed to be in hydrostatic equilibrium along the vertical direction. However, the imposed temperature gradient across the modeled chemical spot quickly generates a horizontal pressure gradient, which initiates lateral flow that facilitates the mixing of cooler and warmer gas regions.

The fixed temperature gradient at the base, representing the stellar surface, likely sustains the circulation flow. This is visually evident in the horizontal flow velocity (middle panels of Fig. 1), where red colour represents lateral motion of the gas to the right and blue represents motion to the left. Likewise, the red colour in the right panel represents upward flow while blue represents downward motion. Thus, alternating red and blue regions indicate continuous flow cycles. The temperature evolution of the left column highlights this circulation further, as pockets of hot gas ascend and then sink back, driven by the established pressure and temperature gradients. The time-scale of the velocity alternation is given by the time during which the flow moves from the centre of the computational domain to its boundaries and bounces back, which is about 30 ks.

Throughout the simulation, typical flow velocities reach magnitudes on the order of 10^5 cm s⁻¹, reflecting the strength of the pressure gradient-driven flow in this non-magnetic setup. The velocities can be estimated from the equation of motion for the subsonic flow $\rho \partial v_x/\partial t = -\partial p/\partial x$, which on the adopted scale of temperature inhomogeneities proportional to the length of the simulation box gives velocities of about $v_x \sim a \sqrt{\Delta T/T_{\rm eff}} \sim 10^5$ cm s⁻¹.

We have not shown the density structures of any of the models as they are essentially typical of hydrostatic atmosphere with exponential distribution which is not affected significantly by small velocity flows here.

3.2. Standard 10 G Horizontal Magnetic Model

Fig. 2 illustrates the time evolution of our standard magnetic model, which includes a 10 G uniform horizontal magnetic field. In this model, the horizontal magnetic field is sufficiently strong to suppress vertical flows, significantly reducing the vertical mixing of gas. However, the magnetic field strength is not high enough to impede horizontal flows, allowing hot gas to spread laterally with speeds around 10⁴ cm s⁻¹. Consequently, while a vertical temperature gradient is maintained, the hot gas is able to diffuse horizontally away from the initial chemical spot, leading to a more uniform temperature distribution across the stellar surface

This behavior contrasts with cases involving stronger magnetic fields (see Table 1), where both vertical and horizontal flows are heavily suppressed. In such high-magnetic field cases, the temperature stratification remains tightly confined to the chemical spot region due to the strong magnetic inhibition of flow. By comparing these cases, we gain insight into how varying magnetic field strengths influence the transport of energy and matter within the atmosphere, with intermediate fields allowing

lateral diffusion while stronger fields create isolated, thermally stratified regions.

3.3. Parameter Study

To assess the general effects of magnetic fields on atmospheric dynamics, Fig. 3 displays horizontal flow velocities across all models at the conclusion of our simulations. In the left column, we present cases with a uniform vertical magnetic field orientation, while the right column shows those with a horizontal magnetic field. The results indicate a clear trend: a strong vertical magnetic field effectively suppresses horizontal flows by stabilizing the atmosphere against lateral motion. In our setup, the magnetic field energy density overcomes gas energy density already for 1 G magnetic field at the top of the photosphere. Therefore, already the vertical field with strength of 1 G can suppress the horizontal flow. In contrast, models with strong horizontal magnetic fields produce a gentle, steady horizontal flow or 'breeze' of approximately 10^4 cm s⁻¹. This horizontal flow may play an important role in diffusing and eroding surface abundance spots, thereby reducing their lifetime.

The pattern for vertical flow velocities, shown in Fig. 4, reveals a nearly opposite behavior. Vertical magnetic fields inhibit horizontal flows but allow for limited vertical motion. However, given that the primary temperature gradient in our simulations is oriented horizontally, the absence of sufficient horizontal flow inhibits effective mixing of hot and cool gas, thereby limiting the formation of strong vertical flows.

This dynamics is further emphasized in Fig. 5, which shows the final temperature distribution for each model. In non-magnetic and weakly magnetized cases (1 and 10 G), horizontal flows facilitate the mixing of hot and cool gas, leading to a more homogenized temperature distribution. In contrast, in models with strong magnetic fields, the initial temperature stratification is largely preserved. Here, the magnetic field prevents substantial lateral mixing, maintaining localized regions of hot and cool gas near the initial configuration (Peterson 1970).

These findings underscore the influence of magnetic field orientation and strength on atmospheric dynamics. Strong vertical fields stabilize the atmosphere laterally, while strong horizontal fields promote diffusion. This magnetic regulation of flow has implications for the persistence and evolution of surface abundance features, particularly in magnetic chemically peculiar stars where such abundance anomalies are often observed.

4. Discussion

Our simulations were calculated for a specific set of stellar parameters corresponding to a particular helium-strong chemically peculiar star. However, the phenomenon studied in this paper is not constrained to this specific set of parameters, but is applicable to all stars with an inhomogeneous surface abundance distribution, albeit with differing strength and timescales. The interplay between radiative diffusion, horizontal flows, and other processes influencing abundance evolution suggests that the underlying mechanisms operate across various stellar types, even though the specific characteristics and evolutionary timescales of abundance inhomogeneities may vary significantly.

In non-magnetic stars of spectral type BA, our simulations presented here estimate the speed of atmospheric flow connected to horizontal temperature inhomogeneities of the order of 10^5 cm s⁻¹ (cf. Sect. 3.1). Taking into an account a typical radius of such star, the mixing timescale is of order of tens of days.

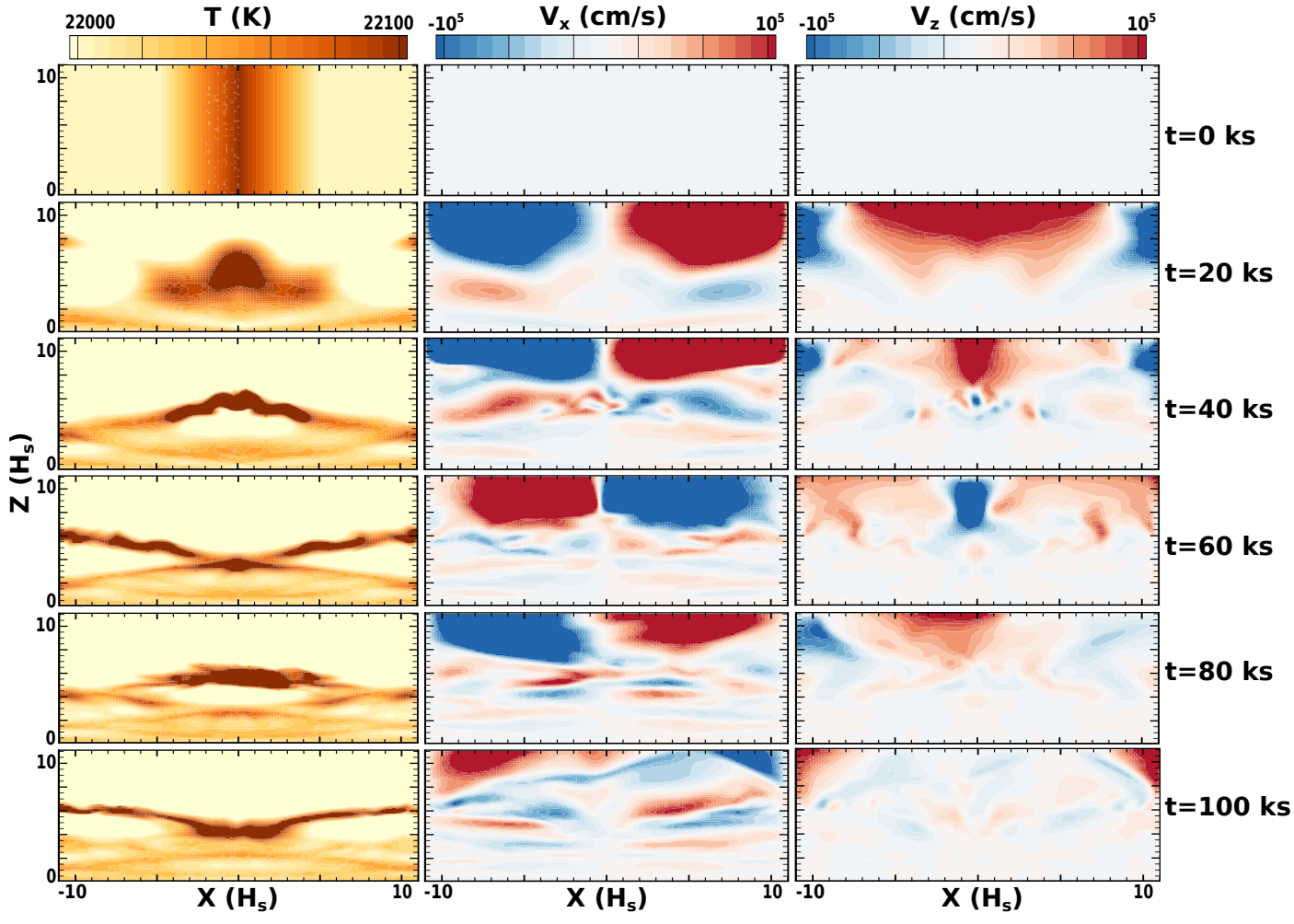


Fig. 1. Time evolution of the non-magnetic model. The top row shows the initial snapshot, with subsequent time snapshots taken every 20 ks. The left column presents temperature in Kelvin, the middle column illustrates horizontal flow velocity, and the right column displays vertical flow velocity in cm s⁻¹.

However, it is conceivable that normal BA stars possess surface magnetic fields with typical strengths of the order of 1 G (Lignières et al. 2009; Petit et al. 2011; Blazère et al. 2020). In such a case the typical flow velocities become order of magnitude lower (cf. Sect. 3.2), leading to a typical flow timescales of the order of years. This corresponds to a typical timescale of the evolution of surface abundance spots in HgMn stars (Briquet et al. 2010; Korhonen et al. 2013), thus highlighting a generally good agreement between our model and observations.

In general, the timescale of the spot evolution is comparable with the radiative diffusion timescale. However, this timescale strongly depends on the location in the atmosphere and on the properties of a particular element such as local relative abundance. Consequently, the radiative diffusion timescale is as short as days in the upper parts of the atmosphere, while it might take centuries in deep photospheric layers (Alecian et al. 2011). For a specific case of mercury in the continuum-forming photospheric regions, the radiative diffusion timescale is comparable to the order of year timescales of horizontal flows. This implies that the photospheric flows and radiative diffusion operate on similar timescales in HgMn stars, therefore, the horizontal flow could be one of the processes that precludes strong abundance anomalies in stars with weak magnetic field. Although such flows may contribute to dynamical evolution of abundance spots, we caution that timescale to build the peculiar abundances could be longer.

This suggests that while the radiative diffusion timescale may be relatively short in certain regions, the actual process of creating abundance inhomogeneities involves additional factors that extend the overall timescale. These factors include complex interactions between photospheric flows and radiative diffusion, as well as the slower processes of element migration and accumulation. As a result, the timescale for the creation of abundance inhomogeneities might be longer than the radiative diffusion timescale alone would suggest. Understanding these extended timescales is crucial for accurately modeling and interpreting the abundance patterns observed in HgMn stars.

For mass-loss rates predicted in a magnetic helium-strong star HD 37776 (Krtička 2014), the wind velocity in the continuum forming regions of the photosphere, which is of the order of $10~{\rm cm~s^{-1}}$, is lower than the velocity of horizontal flows. However, the stellar wind quickly accelerates and overcomes the horizontal flow velocity by one to two orders of magnitude in the upper parts of the photosphere.

On the other hand, our simulations show that magnetic fields stronger than about 100 G inhibit any flow generated by the horizontal temperature gradients. These are typical fields detected in magnetic chemically peculiar stars (Morel et al. 2015; Wade et al. 2016; Grunhut et al. 2017). Therefore, inhibition of horizontal flow by vertical magnetic field contributes to the establishment of abundance anomalies and their stability. Still, even

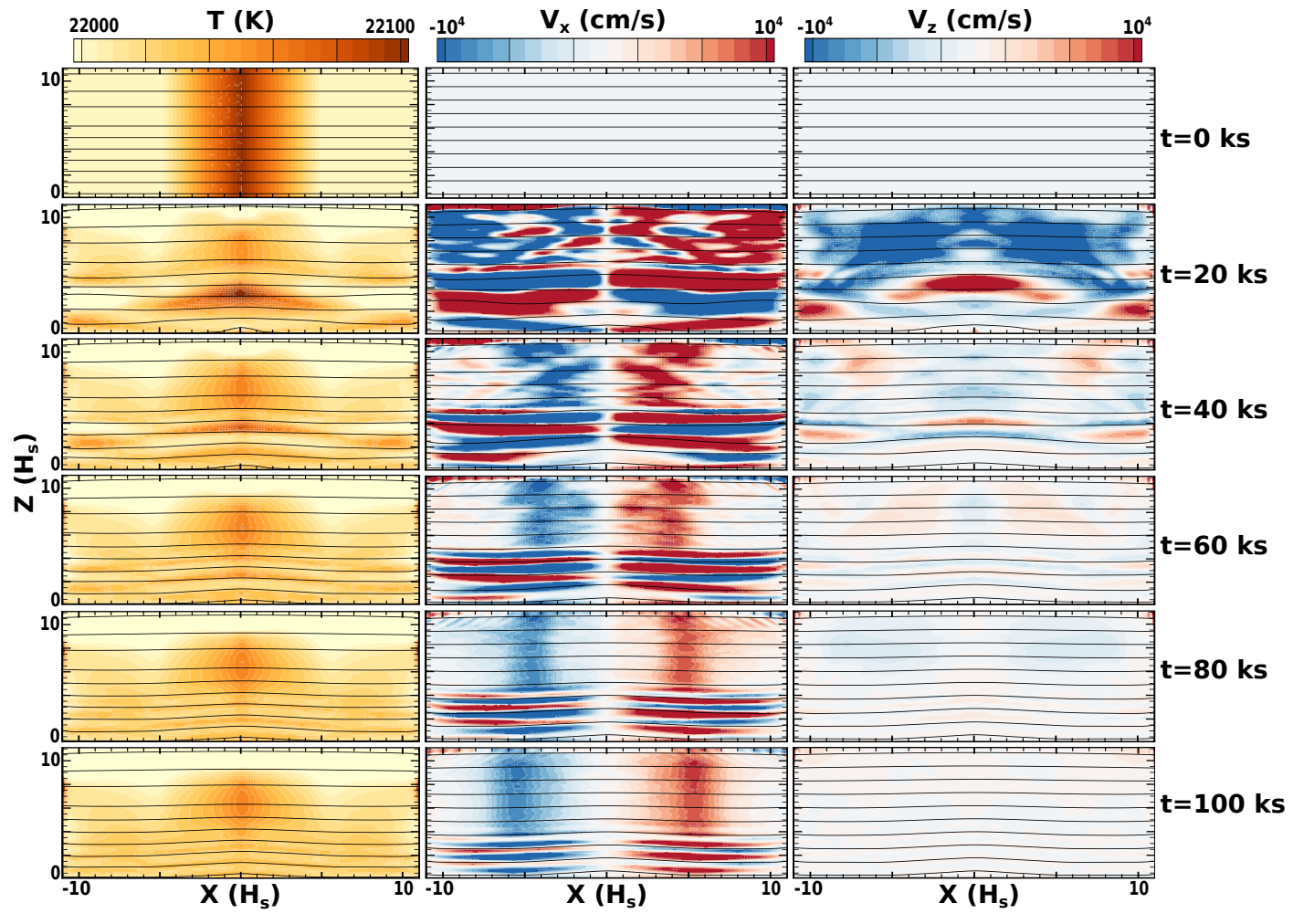


Fig. 2. Time evolution of the standard magnetic model with initial uniform 10 G magnetic field (black lines) in the horizontal direction. The top row shows the initial time snapshot, with subsequent time snapshots taken every 20 ks. The left column shows temperature in Kelvin, the middle column illustrates horizontal flow velocity, and the right column displays vertical flow velocity in cm s⁻¹. Note that the range for velocity is factor 10 lower than for the non-magnetic case in Fig. 1. This highlights the effects magnetic field can have on the atmospheric flow.

in these stars relative rapid flows with speeds of the order of $10^3\,\mathrm{cm\,s^{-1}}$ are possible in the regions with horizontal magnetic fields. Such flow can contribute to the stratification of chemical elements in magnetic chemically peculiar stars.

The atmospheric flows induced by horizontal temperature gradients may reach up to $10^5 \, \mathrm{cm \, s^{-1}}$. Such velocities are in principle at the verge of detection using the method of Doppler imaging. Future observational campaigns might help us verify the predictions of our simulations.

5. Summary and future work

Our study investigates the effects of magnetic fields on atmospheric dynamics in chemically peculiar stars, focusing on how different magnetic field strengths and orientations influence horizontal and vertical flows. The photospheric flows are supposed to originate due to horizontal temperature inhomogeneities connected with abundance stratification. We find that strong vertical magnetic fields inhibit horizontal flows, preserving temperature stratification and stabilizing abundance anomalies. Conversely, strong horizontal magnetic fields enable a lateral 'breeze,' which can erode surface abundance spots over time. In weak or nonmagnetic cases, horizontal flow effectively mixes hot and cool gas, resulting in a more homogenized temperature distribution.

Our results for the flow velocity around $10^4~\rm cm~s^{-1}$, leading to flux timescales of the order of a year, are in good agreement with the typical timescale for the evolution of surface abundance spots in HgMn stars obtained from observations. Our simulations also confirm that the week horizontal flow can contribute to the dynamical evolution of abundance spots in HgMn stars. On the other hand, the strong vertical magnetic field ($\sim 100~\rm G$) can inhibit the horizontal flow and initiate the formation and stabilization of abundance anomalies in chemically peculiar stars.

Future work should expand these simulations to full 3D to capture the complete complexity of flow dynamics and magnetic interactions in stellar atmospheres of chemically peculiar stars. More realistic simulations also require a more detailed treatment of energy equation accounting for the radiative equilibrium. Additionally, relaxing the planar atmosphere assumption and incorporating a more realistic, curved stellar surface will allow us to more accurately model atmospheric flows and temperature distributions. These improvements will provide deeper insights into the evolution of surface abundance features in magnetic chemically peculiar stars.

Acknowledgements. A.u.-D. acknowledges NASA ATP grant number 80NSSC22K0628 and support by NASA through Chandra Award number TM4-25001A issued by the Chandra X-ray Observatory 27 Center, which is operated by the Smithsonian Astrophysical Observatory for and on behalf of

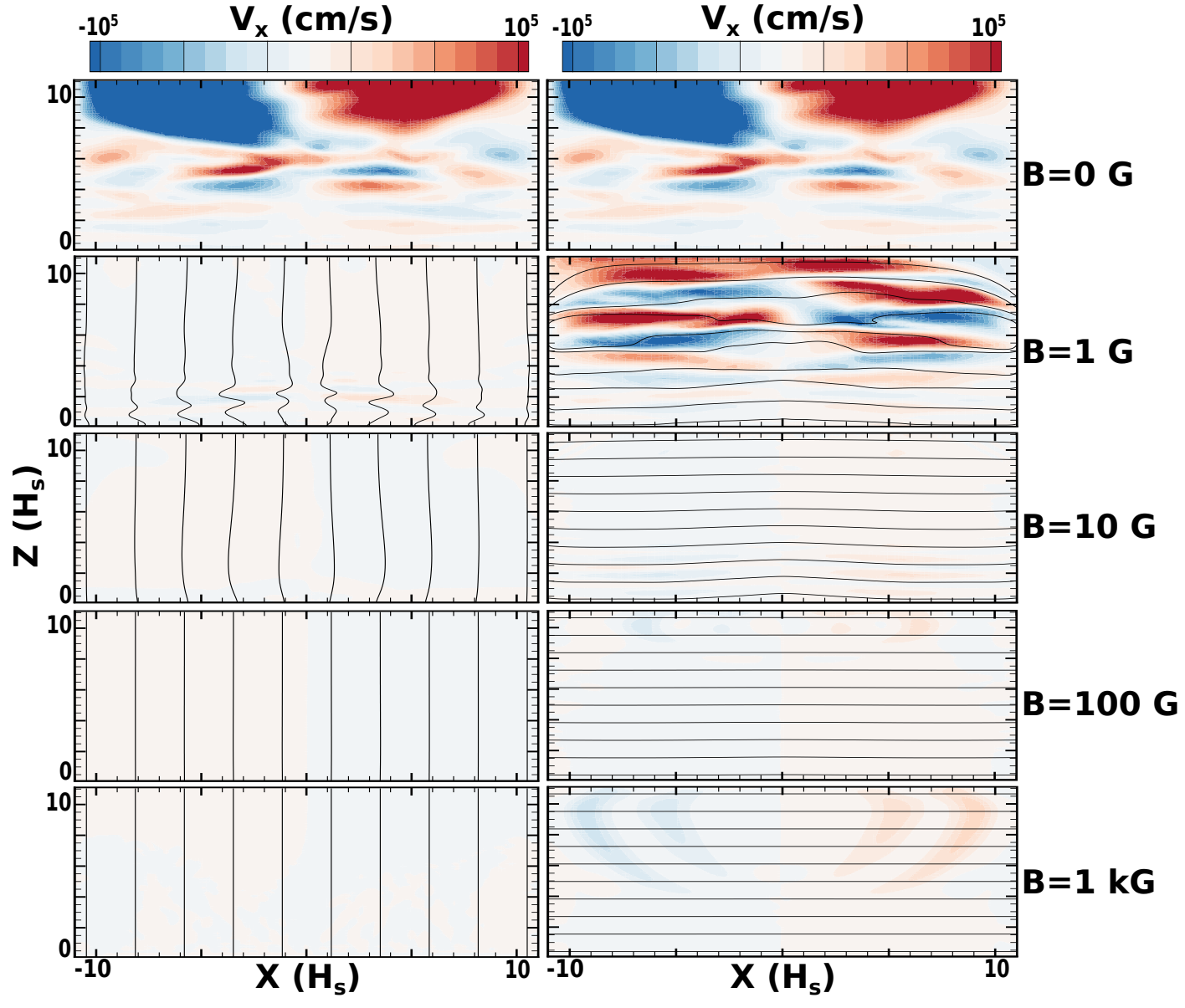


Fig. 3. Horizontal flow velocity for vertical (left column) and horizontal (right column) magnetic field configurations for all the models shown at the final time, t = 100 ks except for the non-magnetic case (top row) shown at time t = 80 ks which is coincidentally more representative than the final time snapshot. The magnetic field strength increases from the top to the bottom.

NASA under contract NAS8-03060. The Astronomical Institute of the Czech Academy of Sciences in Ondřejov is supported by the project RVO:67985815. B.K. acknowledges the support from the Grant Agency of the Czech Republic (GAĈR 22-34467S).

References

Alecian, G. & Stift, M. J. 2017, MNRAS, 468, 1023
Alecian, G. & Stift, M. J. 2019, MNRAS, 482, 4519
Alecian, G., Stift, M. J., & Dorfi, E. A. 2011, MNRAS, 418, 986
Blazère, A., Petit, P., Neiner, C., et al. 2020, MNRAS, 492, 5794
Briquet, M., Korhonen, H., González, J. F., Hubrig, S., & Hackman, T. 2010, A&A, 511, A71
Catanzaro, G., Giarrusso, M., Leone, F., et al. 2016, MNRAS, 460, 1999

Catanzaro, G., Giarrusso, M., Leone, F., et al. 2016, MNRAS, 400, 1999
Das, B., Chandra, P., Shultz, M. E., et al. 2022, ApJ, 925, 125
Faltová, N., Kallová, K., Prišegen, M., et al. 2021, A&A, 656, A125
Fuller, J. & Mathis, S. 2023, MNRAS, 520, 5573
Grunhut, J. H., Wade, G. A., Neiner, C., et al. 2017, MNRAS, 465, 2432
Hayes, J. C., Norman, M. L., Fiedler, R. A., et al. 2006, ApJS, 165, 188

Hümmerich, S., Mikulášek, Z., Paunzen, E., et al. 2018, A&A, 619, A98

Kochukhov, O., Khalack, V., Kobzar, O., et al. 2021, MNRAS, 506, 5328
Kochukhov, O., Lundin, A., Romanyuk, I., & Kudryavtsev, D. 2011, ApJ, 726,
24

Jagelka, M., Mikulášek, Z., Hümmerich, S., & Paunzen, E. 2019, A&A, 622,

Kochukhov, O., Makaganiuk, V., Piskunov, N., et al. 2013, A&A, 554, A61 Kochukhov, O. & Ryabchikova, T. A. 2018, MNRAS, 474, 2787 Kochukhov, O. & Wade, G. A. 2010, A&A, 513, A13

Korhonen, H., González, J. F., Briquet, M., et al. 2013, A&A, 553, A27 Krtička, J. 2014, A&A, 564, A70

Khan, S. A. & Shulyak, D. V. 2007, A&A, 469, 1083

Krtička, J., Mikulášek, Z., Lüftinger, T., & Jagelka, M. 2015, A&A, 576, A82 Krtička, J., Mikulášek, Z., Lüftinger, T., et al. 2012, A&A, 537, A14

Krtička, J., Mikulášek, Z., Luttinger, 1., et al. 2012, A&A, 537, A14 Krtička, J., Mikulášek, Z., Prvák, M., et al. 2020, MNRAS, 493, 2140

Krtička, J., Mikulášek, Z., Zverko, J., & Žižňovský, J. 2007, A&A, 470, 1089 Labadie-Bartz, J., Hümmerich, S., Bernhard, K., Paunzen, E., & Shultz, M. E. 2023, A&A, 676, A55

Leto, P., Trigilio, C., Krtička, J., et al. 2021, MNRAS, 507, 1979 Lignières, F., Petit, P., Böhm, T., & Aurière, M. 2009, A&A, 500, L41 Makaganiuk, V., Kochukhov, O., Piskunov, N., et al. 2012, A&A, 539, A142 Michaud, G., Alecian, G., & Richer, J. 2015, Atomic Diffusion in Stars Michaud, G., Richer, J., & Vick, M. 2011, A&A, 534, A18 Michaud, G., Tarasick, D., Charland, Y., & Pelletier, C. 1983, ApJ, 269, 239

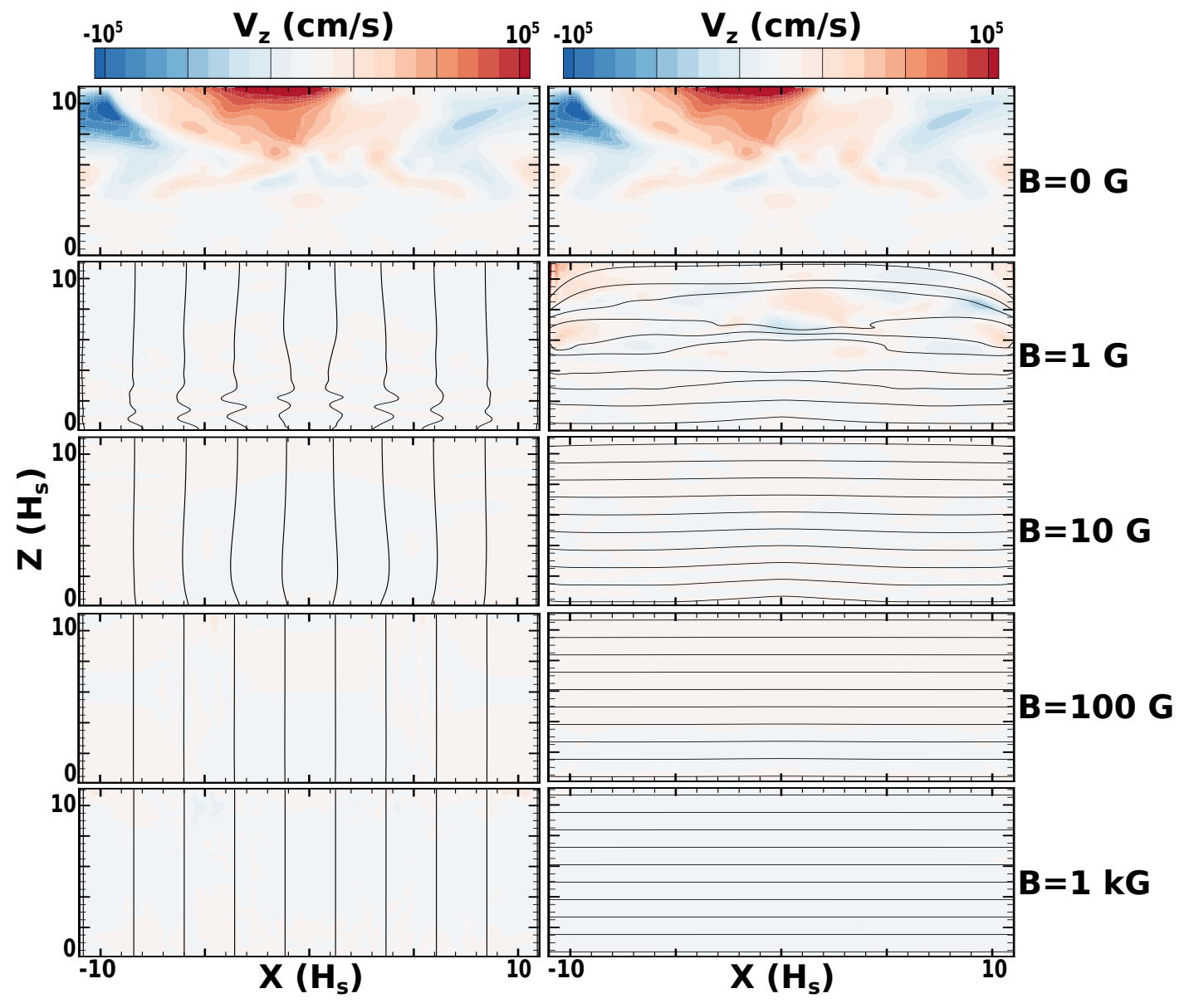


Fig. 4. The same as figure 3 but for radial/vertical flow velocity.

Mikulášek, Z., Krtička, J., Henry, G. W., et al. 2008, A&A, 485, 585 Molnar, M. R. 1973, ApJ, 179, 527

Morel, T., Castro, N., Fossati, L., et al. 2015, in IAU Symposium, Vol. 307, New Windows on Massive Stars, ed. G. Meynet, C. Georgy, J. Groh, & P. Stee, 342–347

Owocki, S. P., Shultz, M. E., ud-Doula, A., et al. 2022, MNRAS, 513, 1449 Peterson, D. M. 1970, ApJ, 161, 685

Petit, P., Lignières, F., Aurière, M., et al. 2011, A&A, 532, L13

Potravnov, I., Piskunov, N., & Ryabchikova, T. 2024, A&A, 689, A111

Prvák, M., Krtička, J., & Korhonen, H. 2020, MNRAS, 492, 1834

Prvák, M., Liška, J., Krtička, J., Mikulášek, Z., & Lüftinger, T. 2015, A&A, 584, A17

Ryabchikova, T., Kochukhov, O., & Bagnulo, S. 2008, A&A, 480, 811

Wade, G. A., Neiner, C., Alecian, E., et al. 2016, MNRAS, 456, 2

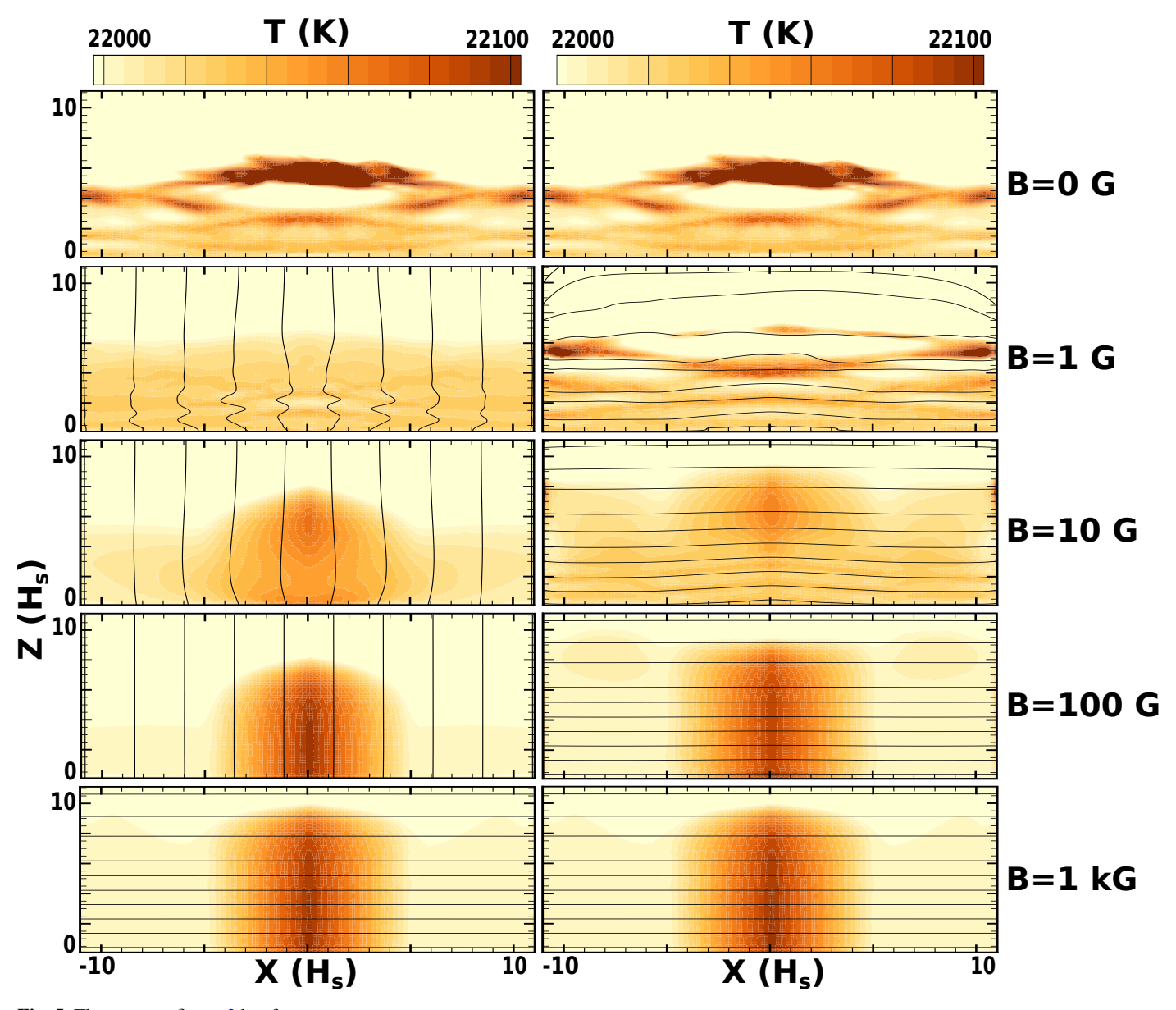


Fig. 5. The same as figure 3 but for temperature.